This pdf file consists of figures containing photographs, and their captions, scanned from:

STRUCTURE OF THE BREVARD ZONE AND BLUE RIDGE NEAR LENOIR, NORTH CAROLINA, WITH OBSERVATIONS ON OBLIQUE CRENULATION CLEAVAGE AND A PRELIMINARY THEORY FOR IRROTATIONAL STRUCTURES IN SHEAR ZONES

by

Andy R. Bobyarchick

A Dissertation

Submitted to the State University of New York

at Albany

in Partial Fulfillment of

the Requirements for the Degree of

Doctor of Philosophy

College of Science and Mathematics

Department of Geological Sciences

1983

FIGURE 2-3. - Sphene grain in amphibole gneiss near Linville Falls fault. The grain lies parallel to foliation and has been separated along fractures now filled mainly with quartz. AB81-30-3, 10X, PPL.

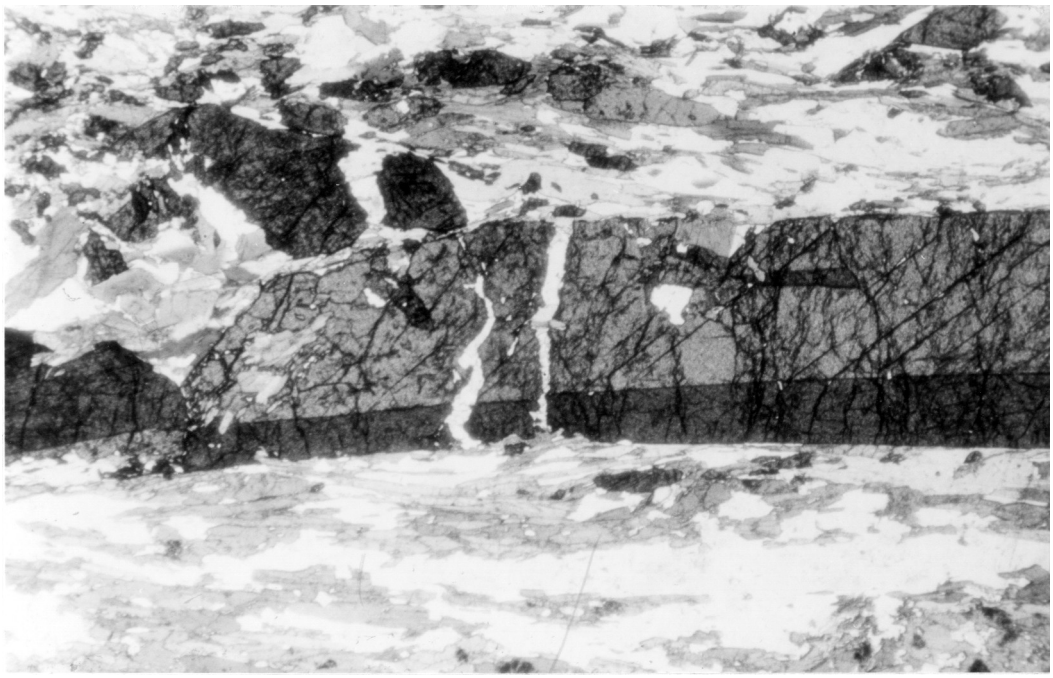

FIGURE 2-3

FIGURE 2-4. - Hornblende grain from lower part of Blue Ridge thrust sheet. The grain contains a turbid core with regularly arranged strings of opaque dust. AB81-30-1, 40X, PPL.

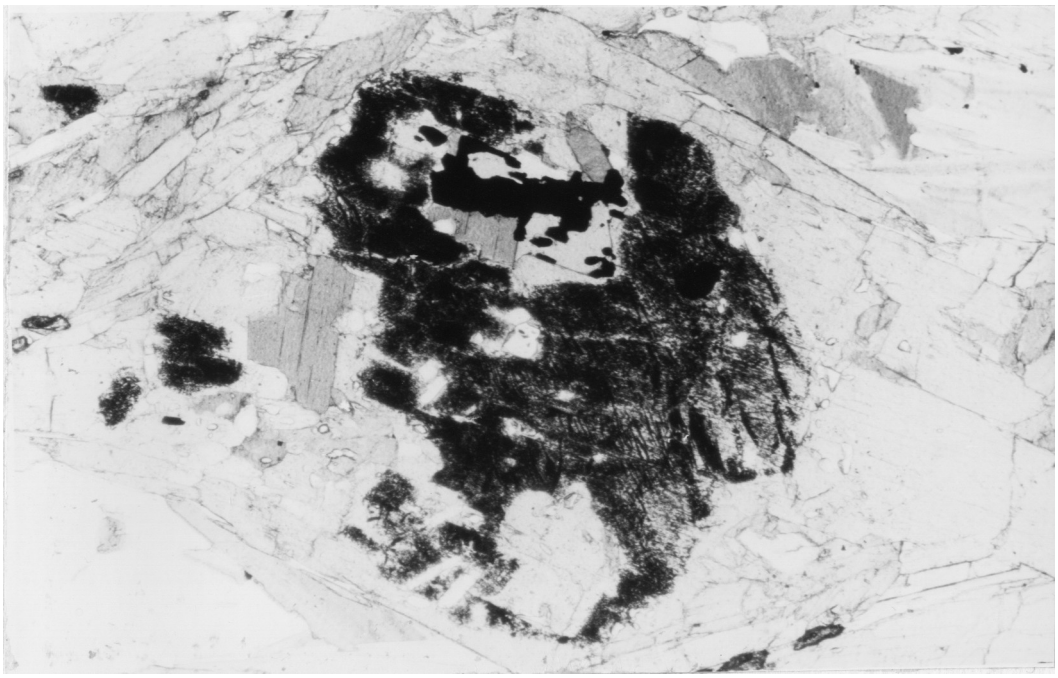

FIGURE 2-4

FIGURE 2-5. - Contorted layering in layered gneiss complex. The outcrop is in Elk Creek near Elkville. Light colored layers are composed of coarse quartz and feldspar with garnet and muscovite. Gray layers are chlorite-muscovite-quartz schist. Where the quartzo-feldspathic layers are tightly folded, competency differences caused the separation of these layers into boudin-like structures. The longest boudin axes could not be determined in the outcrop.

FIGURE 2-5

FIGURE 3-3. - Lineation in phyllonites in the Grandfather Mountain window. The section is an uncut foliation surface on a fine grained chlorite-sericite-quartz phyllite or phyllonite. A lineation is defined by prominent compositional streaking, the alternation of quartz-rich layers and mica-rich layers. Some quartz grains are elongated parallel to the lineation. AB81-7.

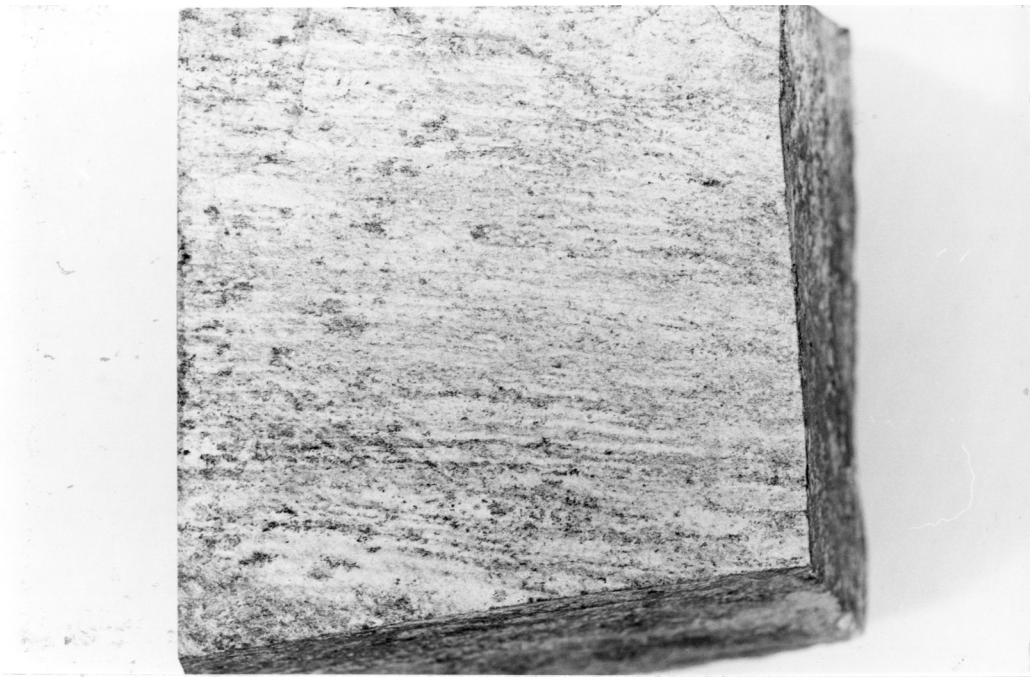

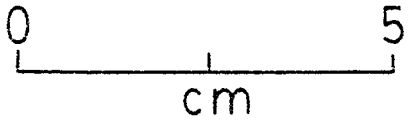

FIGURE 3-3

FIGURE 3-4. - Transposed layering in phyllonites. The sample is the one illustrated in Figure 3-3 but here the cut section is normal to the lineation and normal to the foliation. Quartzose layers are isoclinally folded and disarticulated on the long fold limbs, leading to transposition of compositional layering. The fold hinges are parallel to the lineation and axial surfaces of the folds are parallel to the foliation. AB81-7.

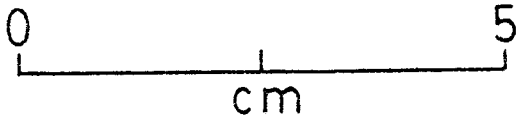

FIGURE 3-4

FIGURE 3-5. - Folded quartzite layers in phyllonite. A. - A view down the plunge of a culmination in a thick quartzite layer. Compositional banding may be original sedimentary layering; heavy mineral, mainly magnetite, streaks are parallel to the banding. Two lobes of the fold verge away from the bisector of the culmination. Such fold styles are rare and may be caused, in part, by soft sediment deformation. B. - Asymmetric, tight folds in layering from a sample near A. Weak cleavage is present in hinge regions of folds. Even here, some quartzite layers are chaotically deformed.

FIGURE 3-5A

FIGURE 3-5B

FIGURE 3-6. - Crenulations in phyllonites. This is the same sample as in Figure 3-3 but here the cut section is parallel to the lineation and normal to the foliation. Very fine crenulations, visible in dark (micaceous) layers, and broader undulations distort the mylonitic foliation.

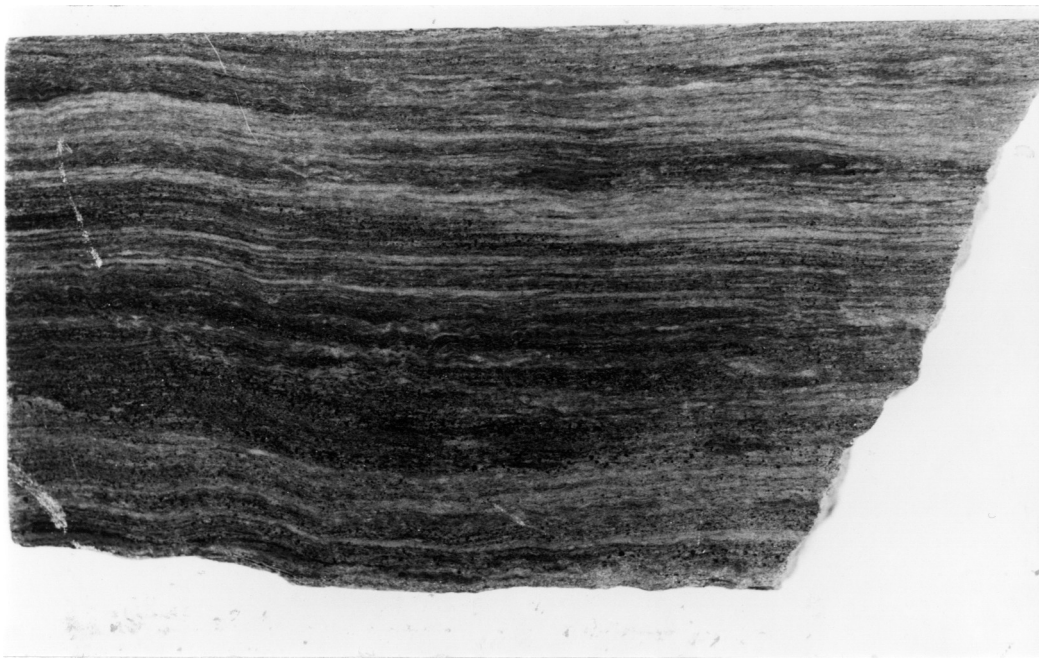

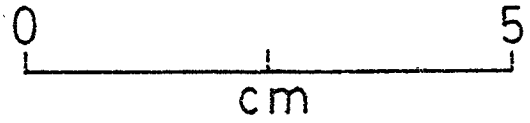

FIGURE 3-6

FIGURE 3-7. - Culminations and saddles in phyllonite. The sample has been cut parallel to the mylonite foliation. Dark gray, sericitic patches underlie the culminations. A finely-spaced lineation (crenulation axes) trends left-right on the cut surface and younger crenulation axes (see Fig. 3-6) trend top-bottom. AB81-9.

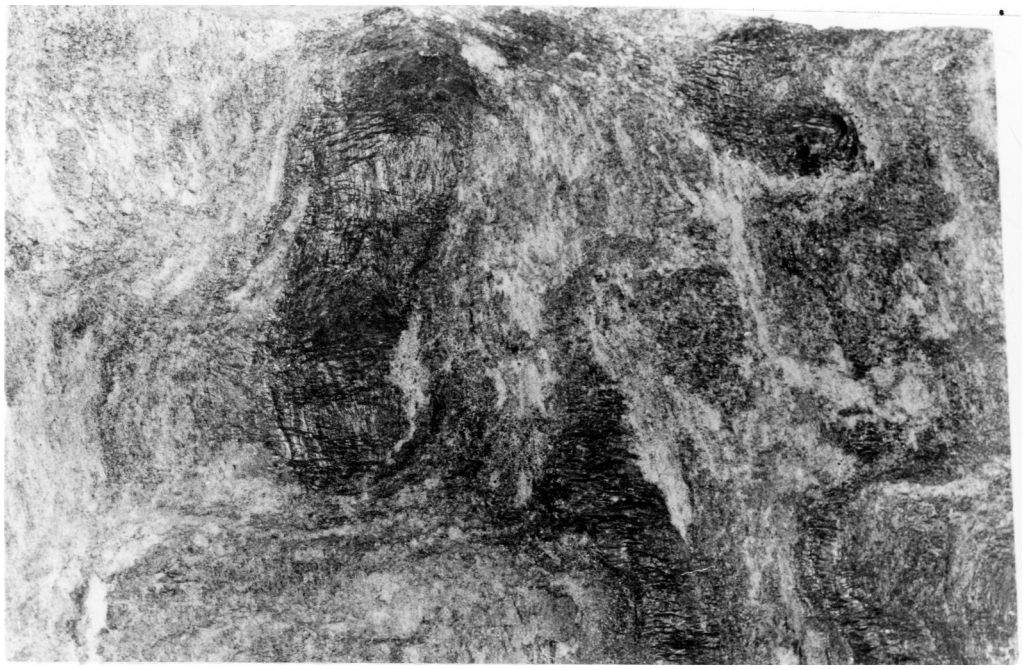

FIGURE 3-7

FIGURE 3-8. - Sericite/chlorite masses in phyllonites. Irregular bright and dark network in the center is the sericite/chlorite mass. Clear, gray or white grains are quartz. AB81-189, 10X, PX.

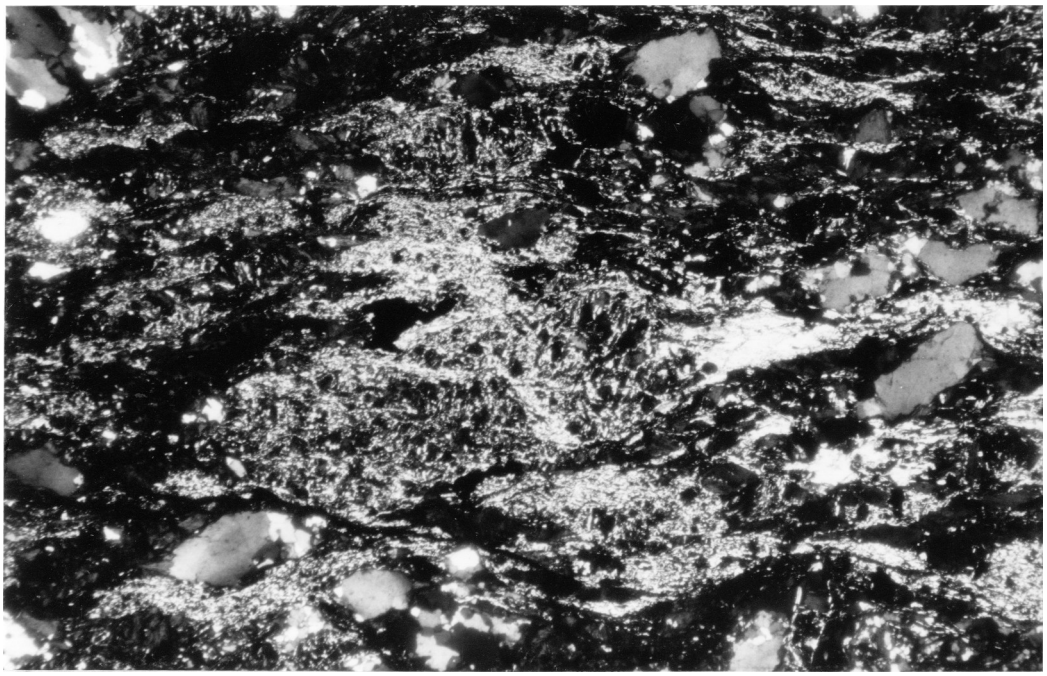

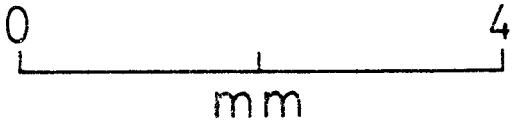

FIGURE 3-8

FIGURE 3-9. - Folding and transposition in phyllonites. A. - Tight folds in a string of opaque minerals (magnetite and pyrite) in phyllonite. The rock is mainly quartz, chlorite, and sericite. AB81-9-2, 40X, partial PX. B. - Sericite layer in phyllonite. Principal mylonite foliation (horizontal) was imprinted on pre-existing foliation or layering. Note gentle crenulations at top. Section normal to mylonite foliation and normal to lineation. AB81-9-2, 40X, PX. C. - Detail of left central part of B. 100X, PX.

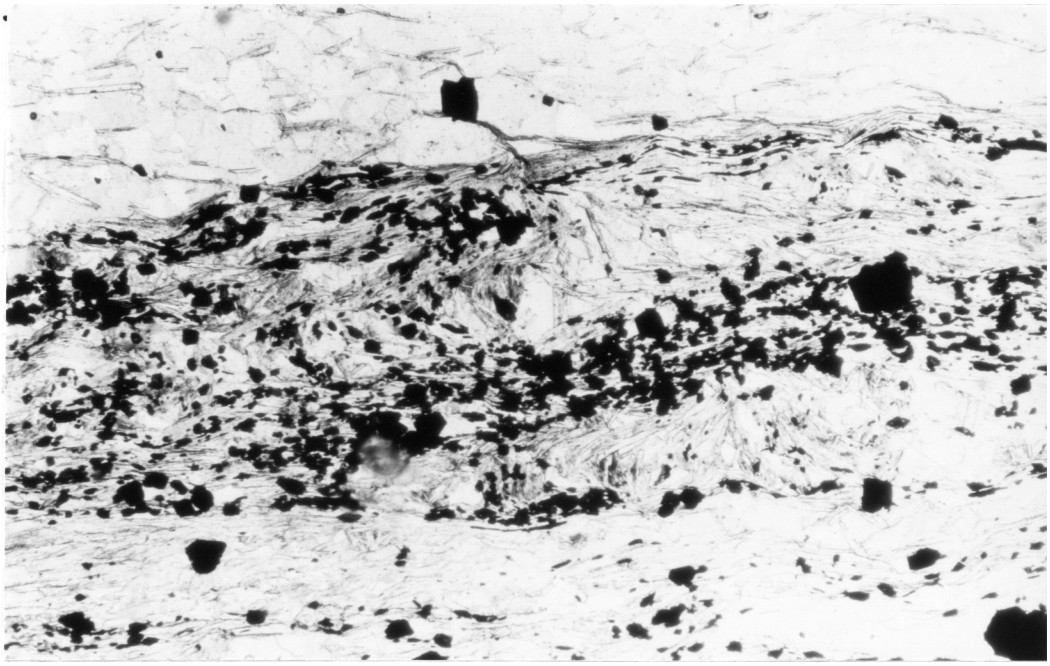

FIGURE 3-9A

FIGURE 3-9B

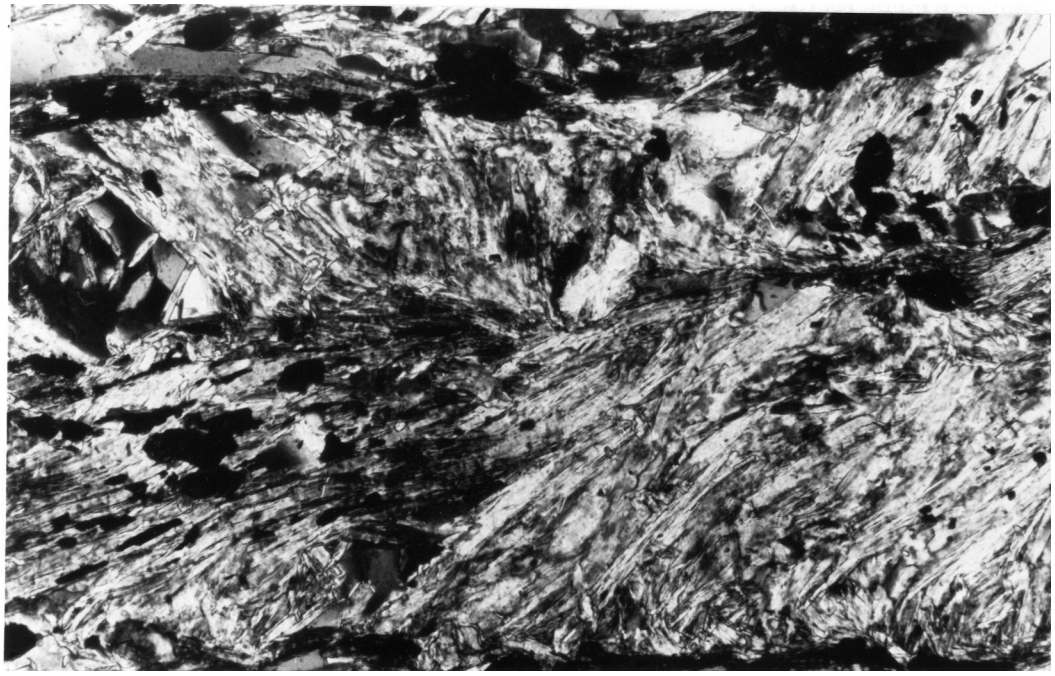

FIGURE 3-9C

FIGURE 3-10. - Pavement outcrop of massive gneiss. The pattern of deformed compositional layering is strongly suggestive of superimposed folding. The hinges of the younger folds plunge moderately to the lower left (south) and roughly down the dip of fold axial surfaces. Older folds are not easy to distinguish; sharp terminations of some micaceous layers may be remnant fold hinges. There is a strong biotite lineation on foliation surfaces that is parallel to the younger fold hinges. The outcrop is in Elk Creek near Darby.

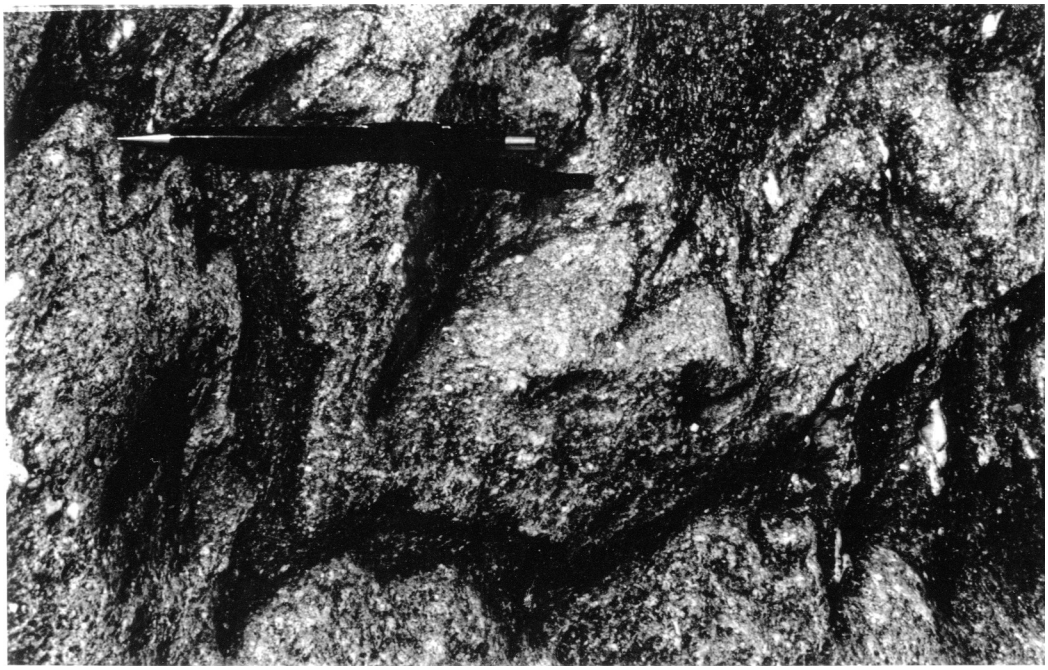

FIGURE 3-10

FIGURE 3-11. - Refolded folds in massive gneiss. Quartzofeldspathic folds in particular show early tight or isoclinal folds later distorted by open or close, asymmetric folds. The outcrop is on an unnamed ridge south of Days Gap, NE Buffalo Cove quadrangle.

FIGURE 3-11

FIGURE 3-12. - Contoured stereoprojections of foliations. All diagrams are lower hemisphere equal-area projections with contour intervals at (0.8), (1.0), 2.0, 6.0, and 14 percent. A. - Poles to principal foliation in Grandfather Mountain window, including mylonite foliation in phyllonites and schistosity in layered rocks and massive gneiss. n = 131. B. - Poles to principal foliation in Blue Ridge thrust sheet between Linville Falls fault and Winding Stairs Mountain fault. n = 103. C. - Poles to principal foliation in Laytown belt. n = 48. D. - Poles to principal foliation in Inner Piedmont. n = 42. Open dots represent mineral elongation lineations. E. - Poles to cleavage in Blue Ridge thrust sheet. n = 59. F. - Poles to mylonite foliation in Brevard zone. n = 127. (In back pocket).

FIGURE 3-13. - Refolded folds in amphibolite layer from Linville Falls fault zone. Amphibolite layers in the outcrop occur as lenses and in the lenses the fold patterns exhibited here are characteristic. Felsic layers were first isoclinally folded then tightly refolded. The axial surfaces of the second folds are sub-parallel to the predominent outcrop foliation. The outcrop lies on the northern flank of an unnamed ridge south of Elk Creek about one mile SE of Darby, NW Grandin quadrangle.

FIGURE 3-13

FIGURE 3-14. - Folds near the Linville Falls fault. A. - Isocline in plagioclase gneiss. Very fine compositional layering is folded. Elsewhere, pre-existing isoclinal folds of this layering have been refolded by folds like the one shown here. Outcrop on Darby Road south of Darby. B. - Similar folds of layered gneiss. Note how the fold height varies with layer thickness. The outcrop is isolated along Darby Road north of the outcrop in A and it is not known if the folds in B are of the same generation as A. C. - Strongly transposed layering in the lower part of the Blue Ridge thrust sheet just south of the Linville Falls fault on Buffalo Cove Road. Folds in felsic layers are disarticulated along their long fold limbs. Feldspar augen in the gneiss may be remnant layering instead of porphyroblasts.

FIGURE 3-14A

FIGURE 3-14B

FIGURE 3-14C

FIGURE 3-15. - Porphyroclastic minerals in the Linville Falls fault. A. - Hornblende porphyroclast with inclusions of plagioclase and biotite. AB82-28, 25X, PX. B. - Plagioclase porphyroclast. The core is intensely epidotized and tails on either side of the core are mainly clear plagioclase with quartz. Note the good internal foliation. AB82-28, 25X, PX. C. - Detail of a plagioclase grain from sample AB82-28. Most clear blobs are also plagioclase. Biotite and epidote inclusions do not cut across the clear plagioclase masses, suggesting that the internal foliation predates them. 25X, PX.

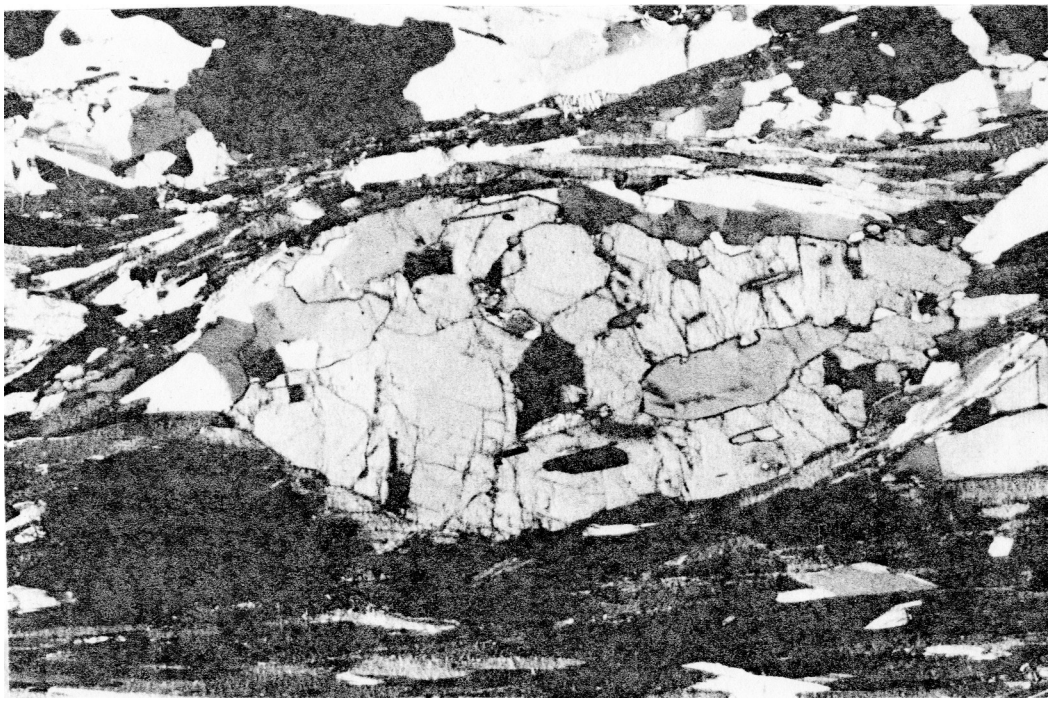

FIGURE 3-15A

FIGURE 3-15B

FIGURE 3-15C

FIGURE 3-16. - Folds in foliation in the Blue Ridge thrust sheet. There is some suggestion in the lower center and upper left parts of the slab that isoclines folding the felsic layers have been refolded by tight folds verging left (northwest). Superimposed folds of this style, with axial planar cleavage locally, characterize shear zones and faults within the thrust sheet.

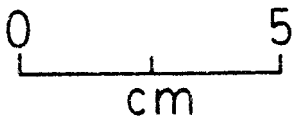

FIGURE 3-16

FIGURE 3-17. - Rootless isoclines in the Laytown belt. The unusually regular compositional layering in rocks like this in the Laytown belt is suggestive of transposed layering. This polished section is cut normal to schistosity are parallel to a mica lineation. Isolated fold hinges in felsic layers (upper left) support the assumption of layer transposition.

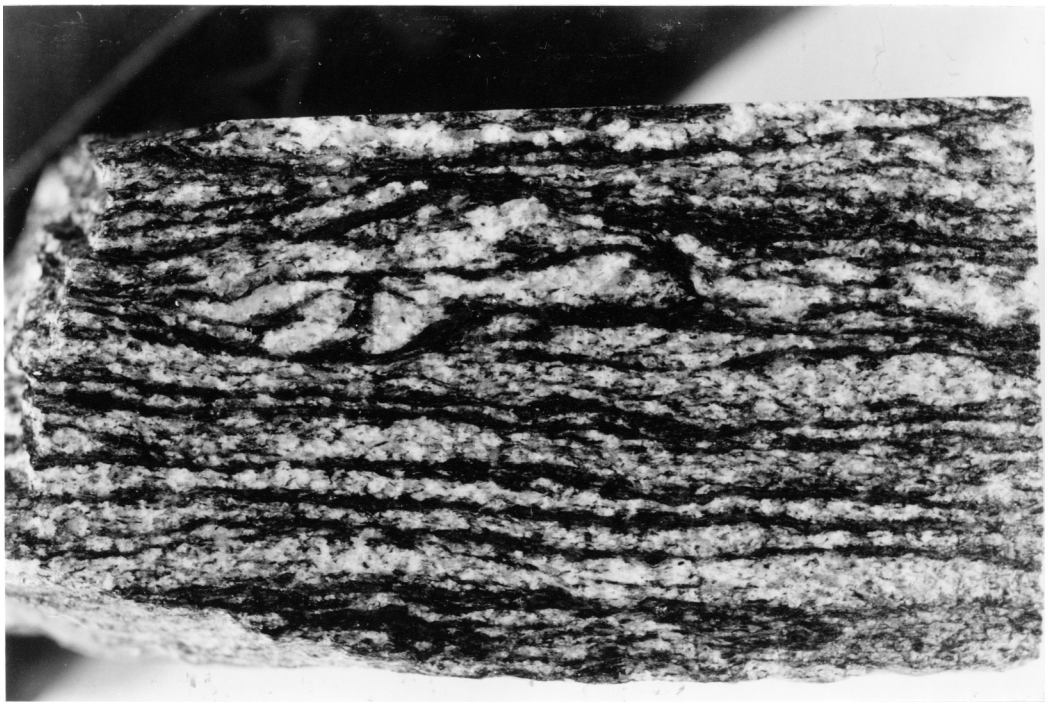

FIGURE 3-17

FIGURE 3-18. - Ripshin Mountain mylonites. A. - Flattened plagioclase porphyroclasts have their long dimensions (in this photograph) parallel to the mylonite foliation (horizontal). Note that polysynthetic twinning commonly stands at a high angle to the foliation. AB82-74, 25X, PX. B. - Oblique crenulation cleavage in Ripshin Mountain mylonite. Cleavage (lower left to upper right) cuts a strong shape fabric at about 20 degrees. AB81-48, 25X, partial PX.

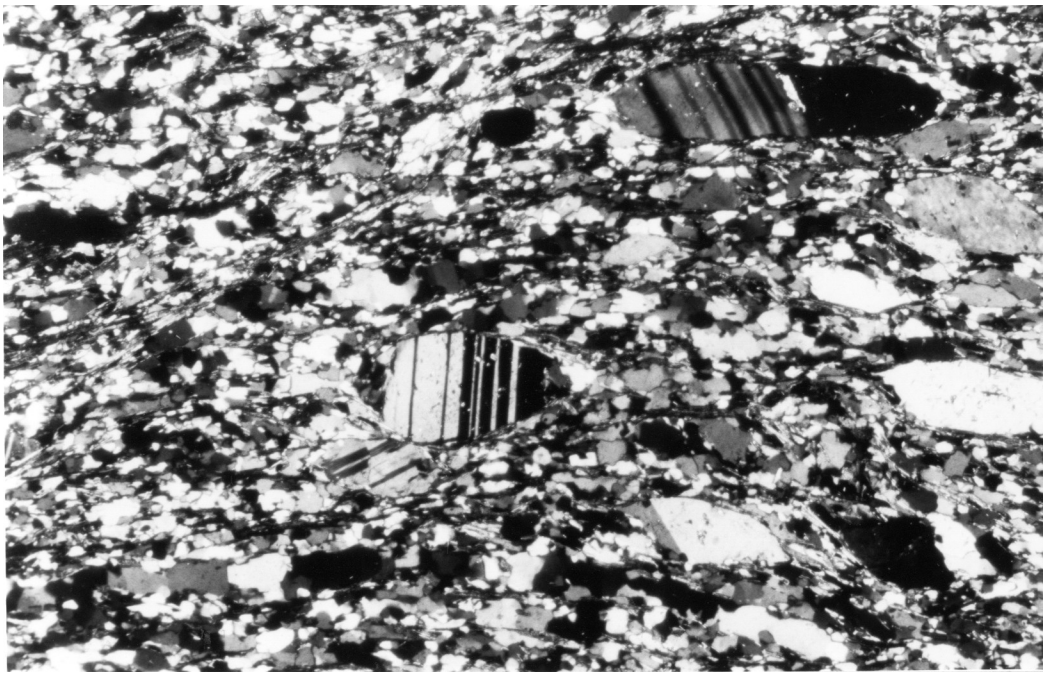

FIGURE 3-18A

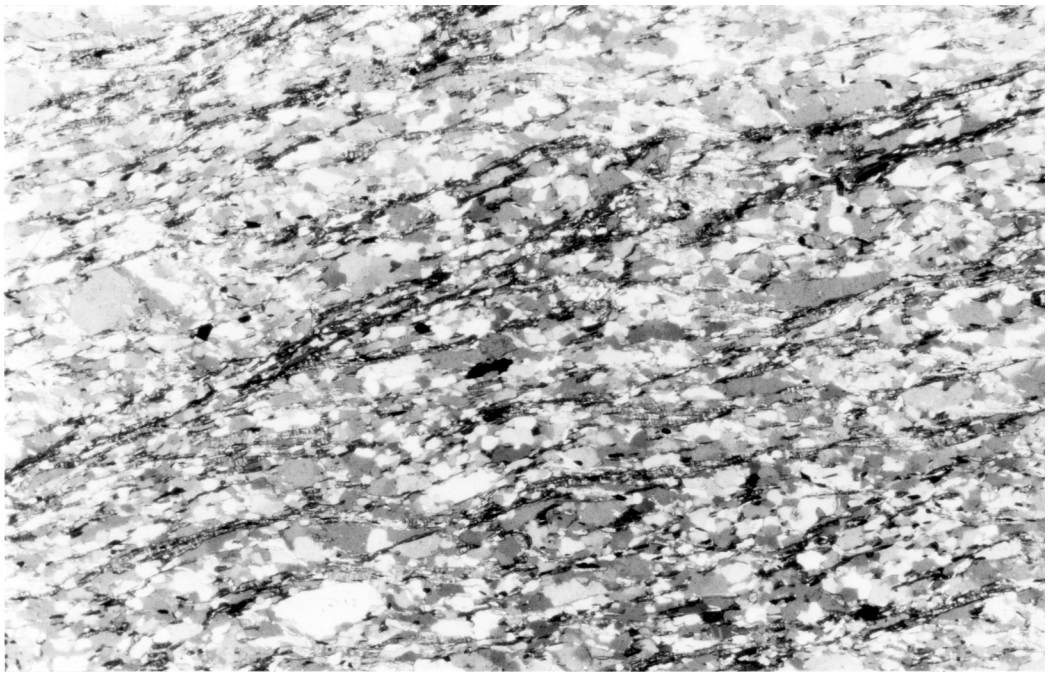

FIGURE 3-18B

FIGURE 3-19. - Layering in quartzite/schist unit. Light colored layers are composed mainly of quartz with minor plagioclase and garnet whereas the dark layers are mainly muscovite, chlorite, garnet and quartz. Layer boundaries are sharp. Irregular white lenses in the schist layers are isoclinally folded quartzites. The outcrop is a large exposure in a sharp bend in Buffalo Creek south of the trend of the Ripshin Mountain fault, SE Buffalo Cove quadrangle.

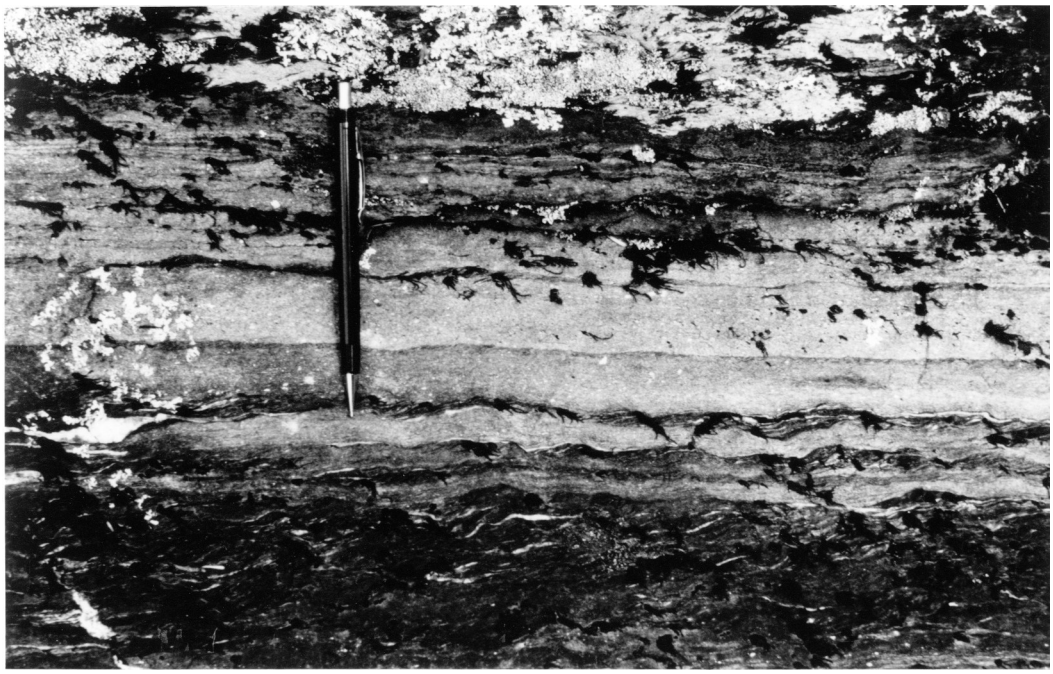

FIGURE 3-19

FIGURE 3-20. - Isoclinally folded quartzite layers in mylonitic schist. (Refer to Fig. 3-19). Wavy undulations in the mylonitic foliation and in the axial surfaces of isoclines is a result of oblique crenulation cleavage. The outcrop is the same as that described in Figure 3-19.

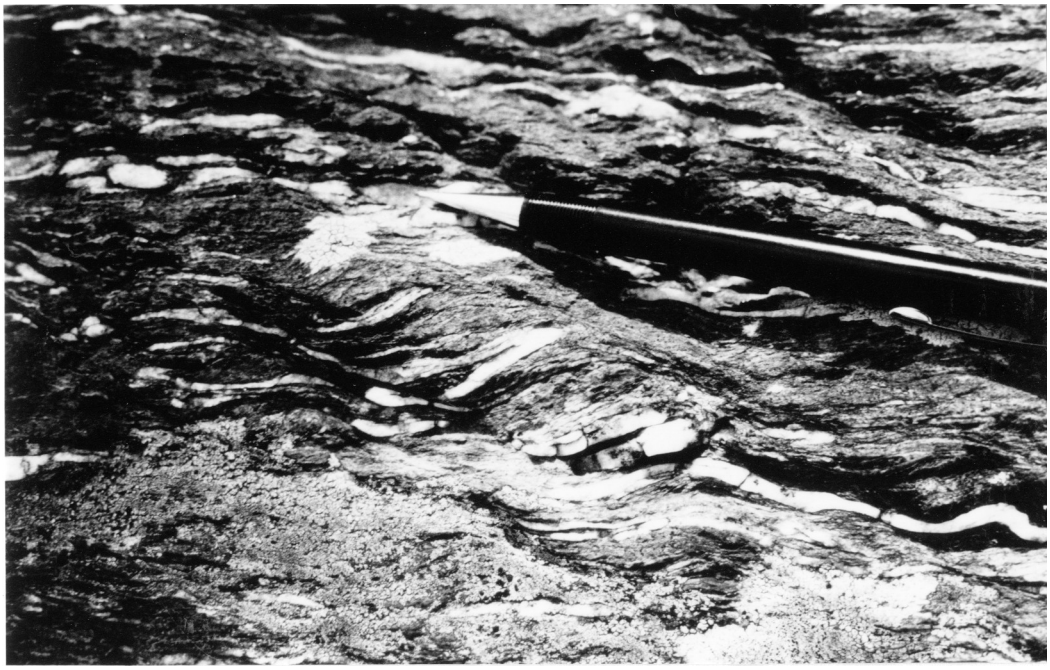

FIGURE 3-20

FIGURE 3-22. - Microscopic isoclinal folding revealed by opaque inclusions. Elsewhere rocks this deformed can often be found with two sets of isoclinal folds. Note curved internal foliation in non-chloritized garnets. AB81-50-X, 25X, PPL.

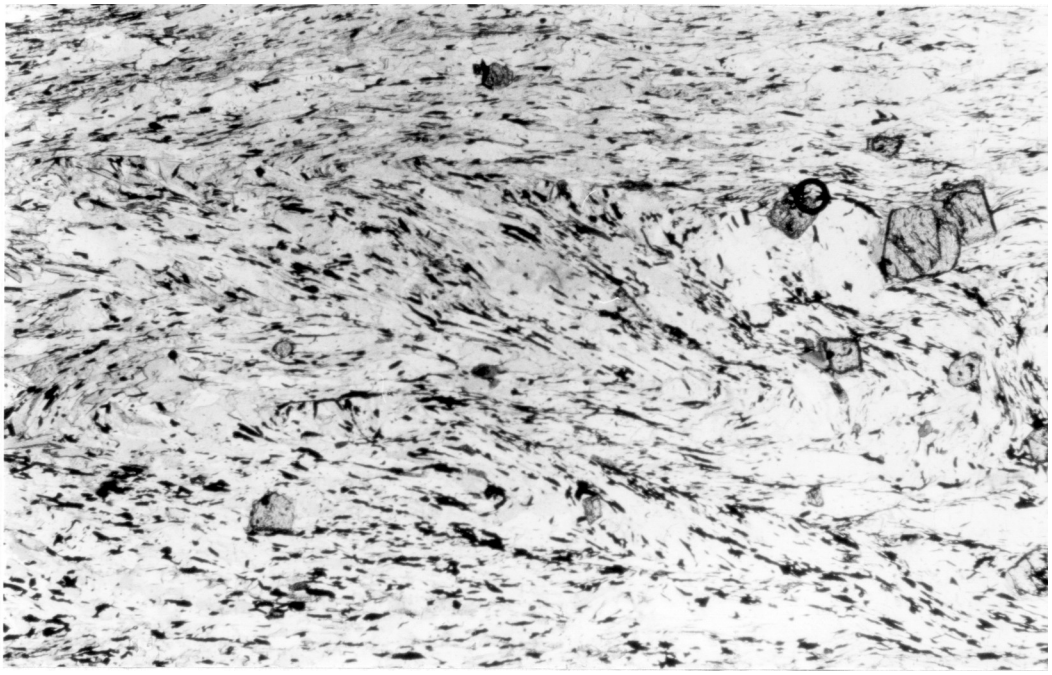

FIGURE 3-22

FIGURE 4-1. - Geometry of oblique crenulation cleavage. OCC - oblique crenulation cleavage; MFES - mylonite foliation enveloping surface; OCL - oblique crenulation limb; CB - crenulation bisector. The mylonite foliation is consistently bent in a sinistral sense across oblique cleavage. The outline of the specimen is a natural fracture surface. Note that there is a tendency for the rock to break parallel to the mylonite foliation or to the oblique cleavage. Figure 4-1A is a sketch of Figure 4-1B.

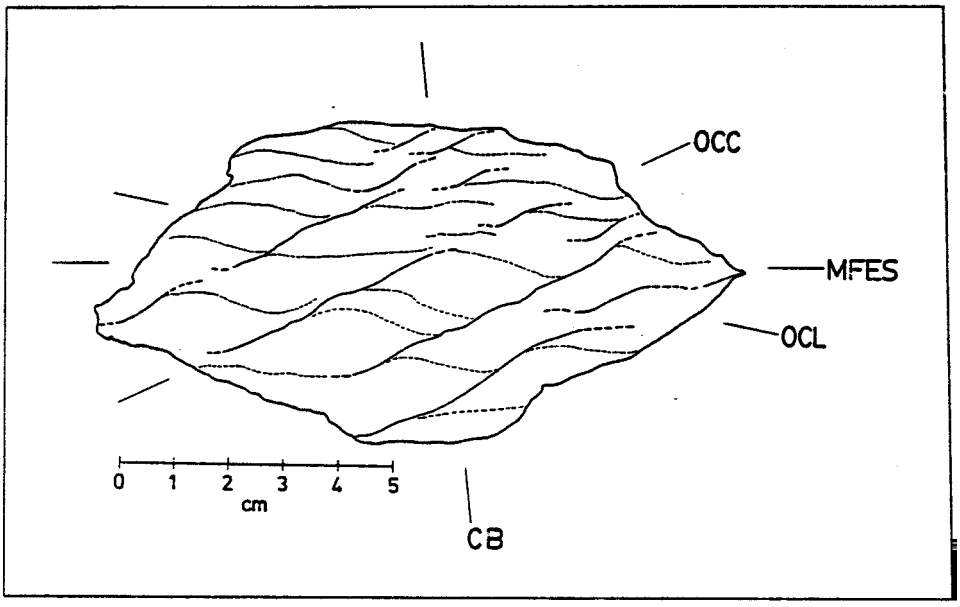

FIGURE 4-1A

FIGURE 4-1B

FIGURE 4-5. - Phacoidal textures in the Brevard zone. A. - Asymmetric phacoids of mica schist interlayered with muscovite-quartz gneiss. The plane of the photograph is about normal to the mylonite foliation. Quartzite layers in the schist show extreme thinning between phacoids. B. - Phacoidal texture in coarse mica schist imparted by oblique crenulation cleavage. The cleavage dips toward the lower right corner of the photograph.

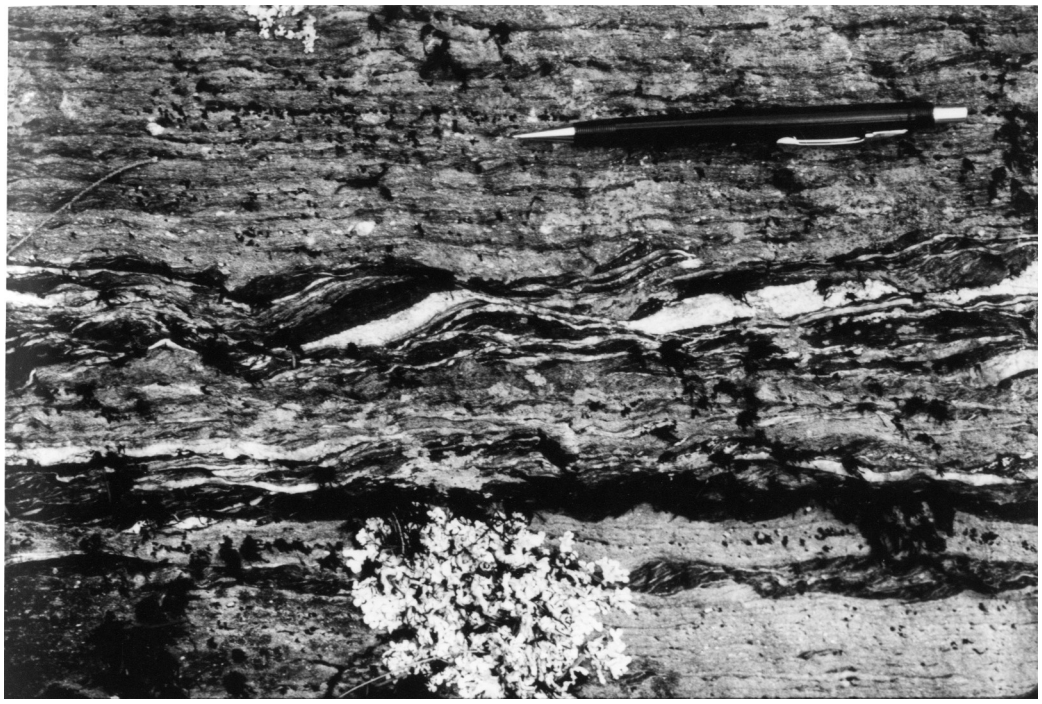

FIGURE 4-5A

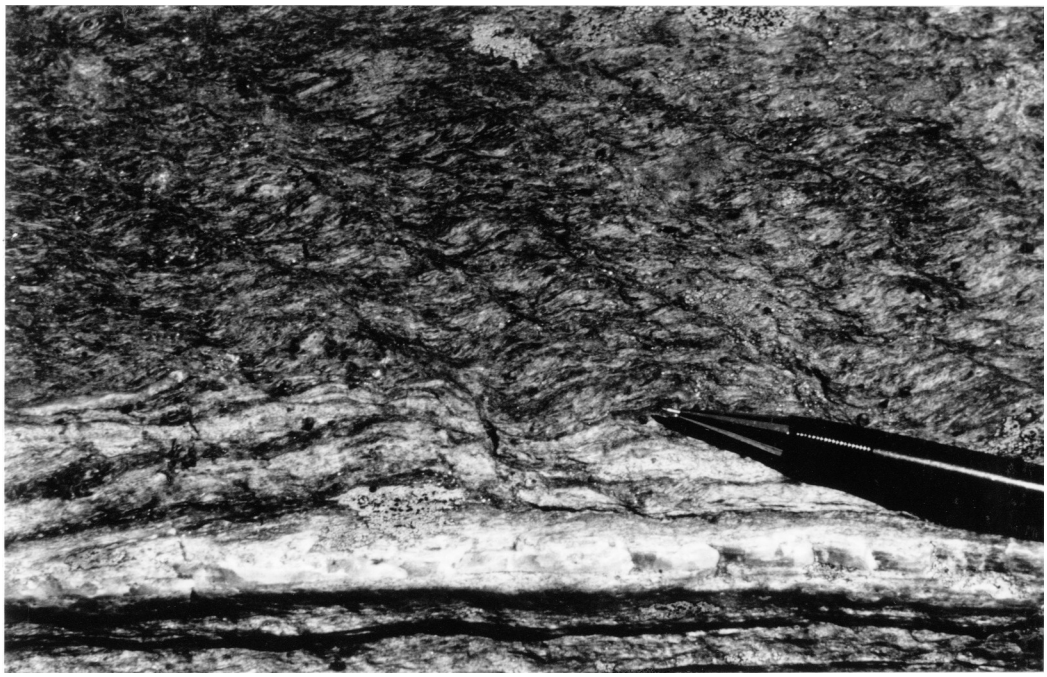

FIGURE 4-5B

FIGURE 4-6. - Ductile faults in Brevard zone mylonites. A. - Sheared quartzite layer similar to the one shown in Figure 4-5A. No distinct fault extends into gneiss on either side of the schist layer. B. - Ductile fault cutting across mylonite foliation and compositional layering in the Brevard zone. The fault is sharp, only about 1 cm across, but layering is continuous across the shear zone. Note that a weak oblique cleavage is present in light colored gneiss in the lower right corner of the photograph.

FIGURE 4-6A

FIGURE 4-6B

FIGURE 4-7. - Photomicrographs of oblique crenulation cleavage. A. - Cleavage in "button" schist. The clear white or gray grains are quartz and platy grains are muscovite. The muscovite grains occur in phacoidal lenses forming "buttons". Oblique is dark because of the presence of opaques and chlorite. AB82-190, 25X, PPL. B. - Same view as A but through crossed polarizers. 25X, PX. C. - Detail from B. A shape orientation in the oblique cleavage is defined by elongate quartz and mica. 100X, PX. D. - Anastomosing cleavage and isoclinally folded muscovite - and quartz-rich layers. Look closely for fold hinges in quartz layers. AB82-190, 10X, PX.

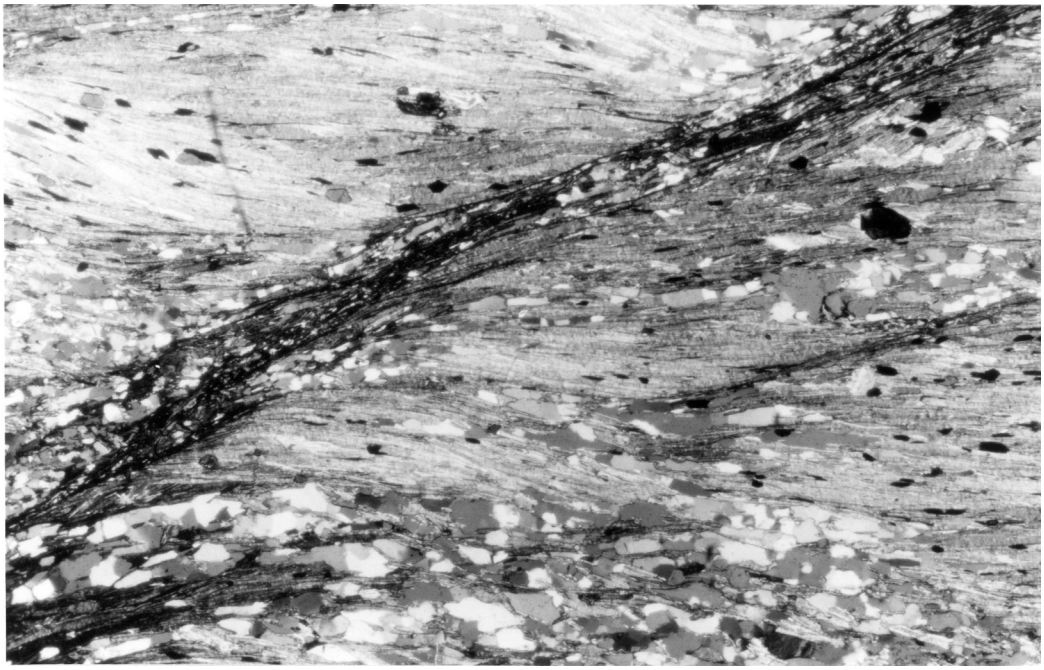

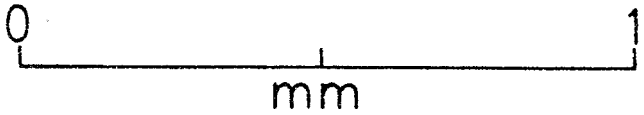

FIGURE 4-7A

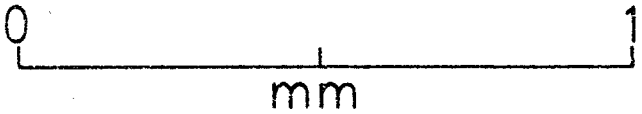

FIGURE 4-7B

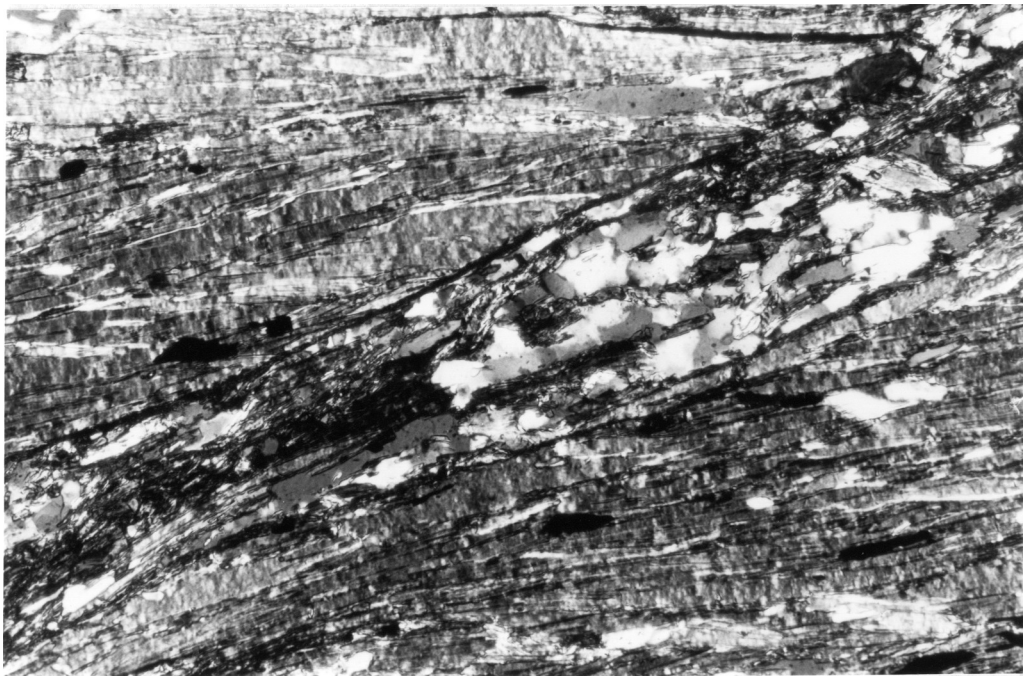

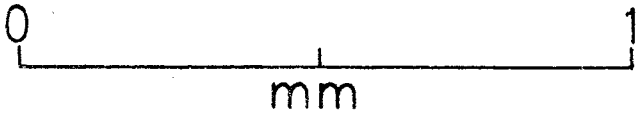

FIGURE 4-7C

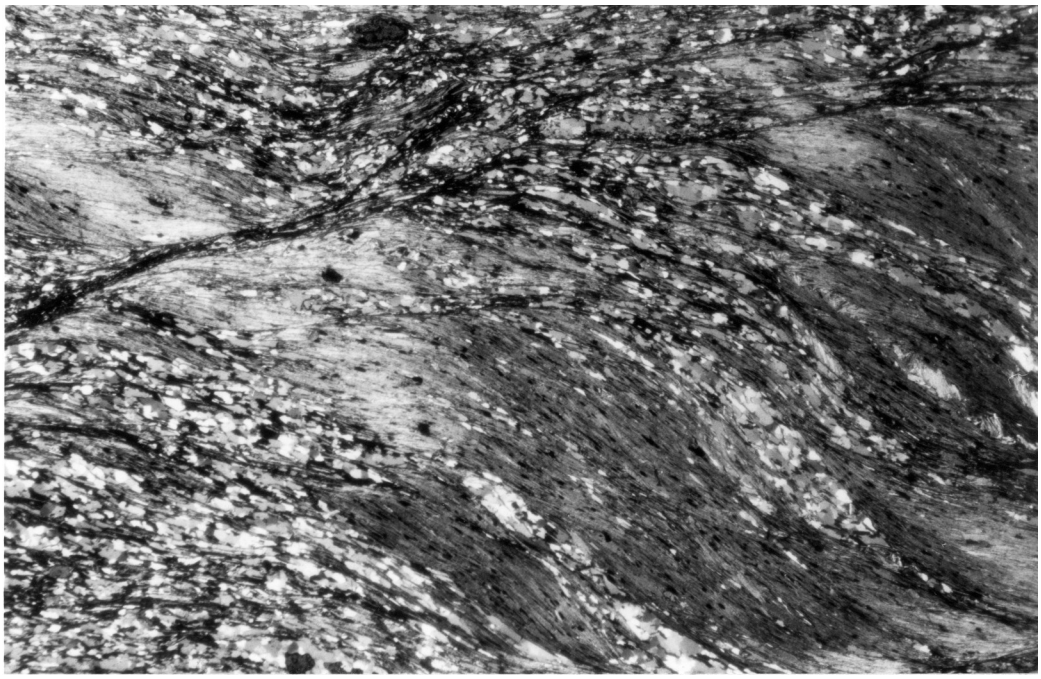

FIGURE 4-7D

FIGURE 4-8. - Chloritized garnet. An irregular core of poikiloblastic garnet is surrounded by a chlorite rim. Note that opaque inclusions defining an internal foliation in the core suffer no deflection in orientation in the chlorite rim. AB81-54A-3, 40X, PPL.

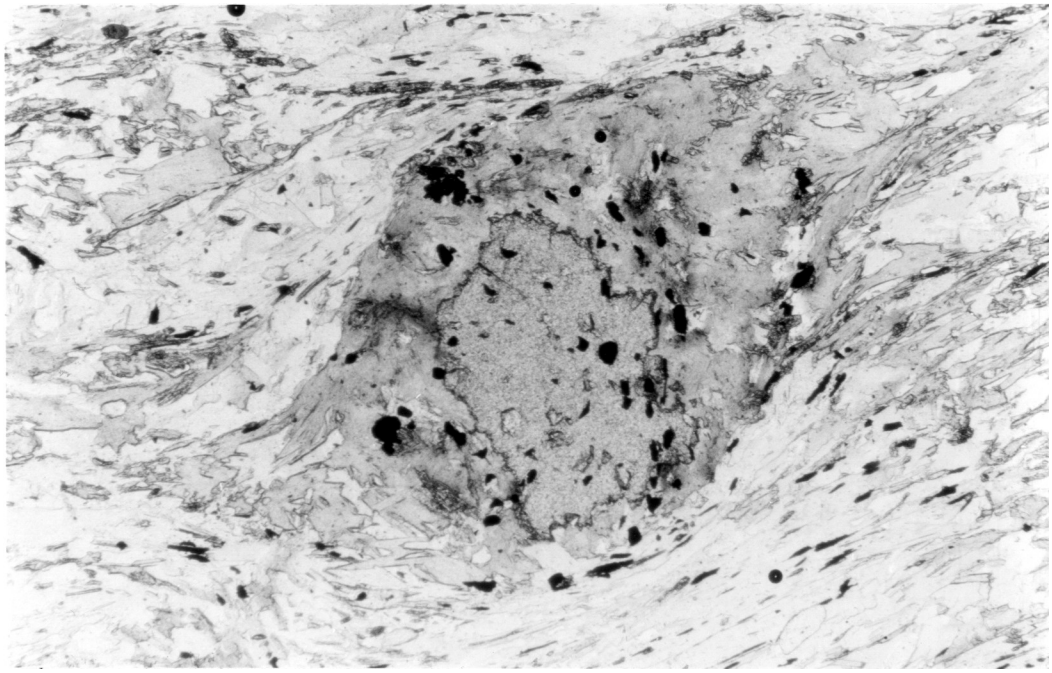

FIGURE 4-8

FIGURE 4-9. - Grain size and shape variations in quartzite layer. A. - Orthogonal quartz grain boundaries in vein enclosed by sericite. AB82-193, 40X, PX. B. - Typical quartz vein microstructure where vein is not near cleavage zone. AB82-193, 25X, PX. C. - Continuation of same vein near cleavage zone. 25X, PX. D. - Trace of same vein in cleavage zone. 25X, PX. E. - Detail of left center part of vein in D. Note numerous subgrains. 100X, PX.

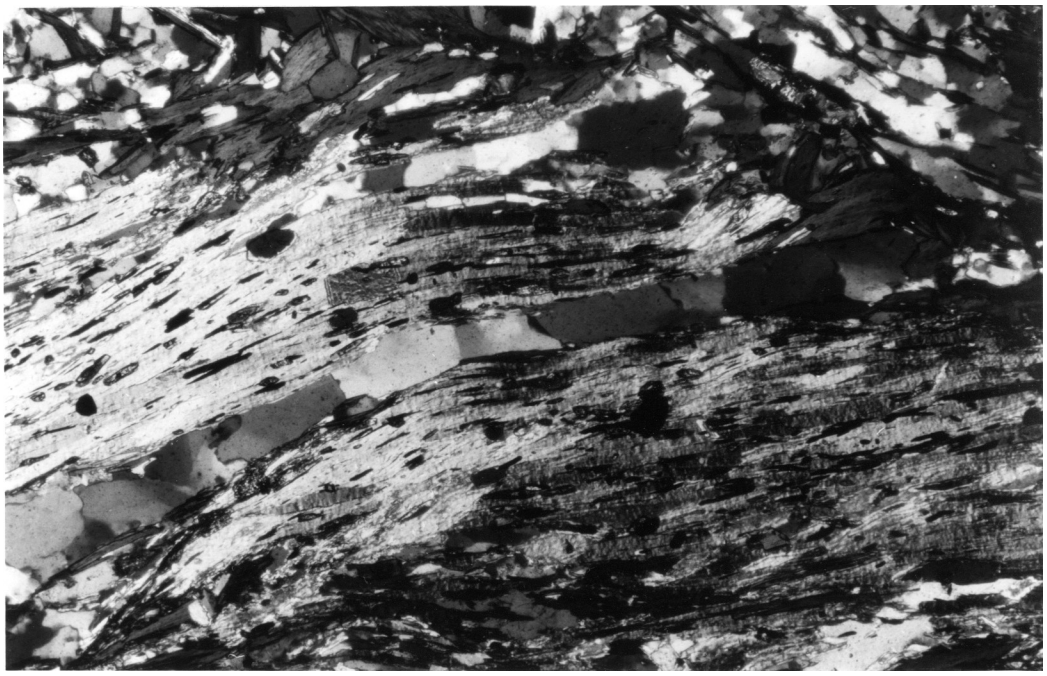

FIGURE 4-9A

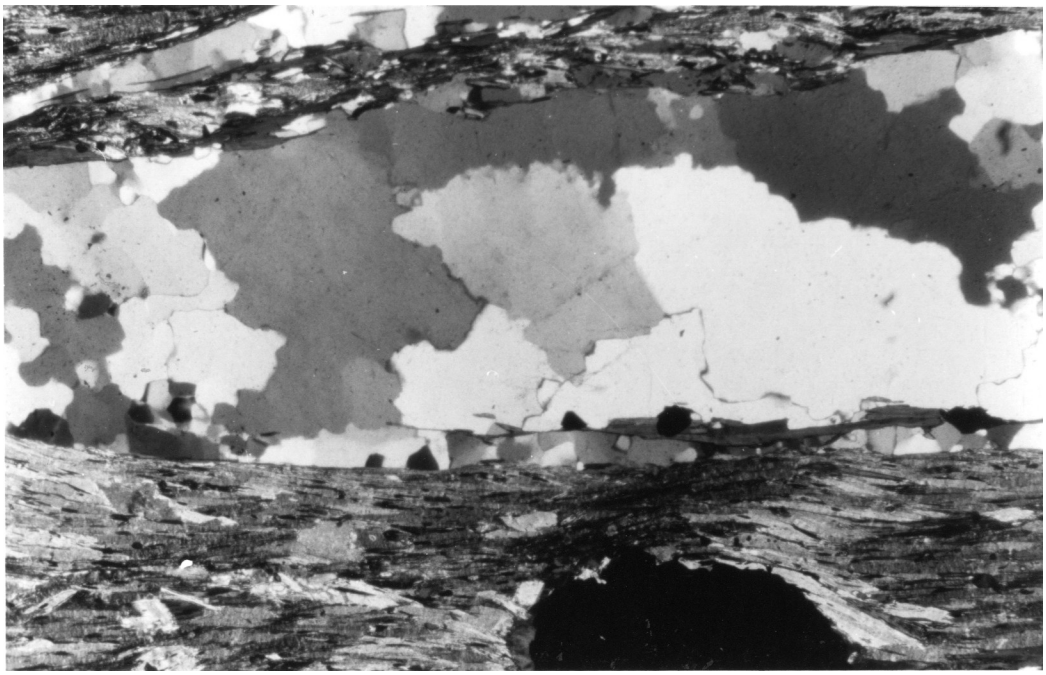

FIGURE 4-9B

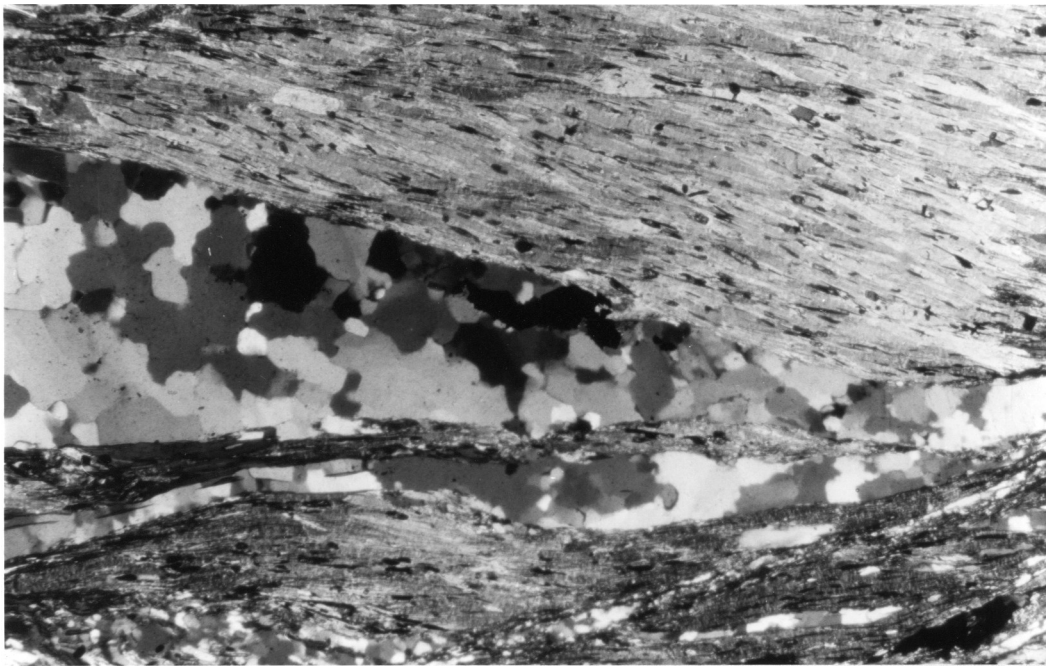

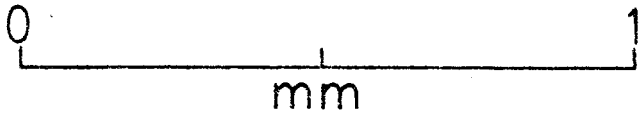

FIGURE 4-9C

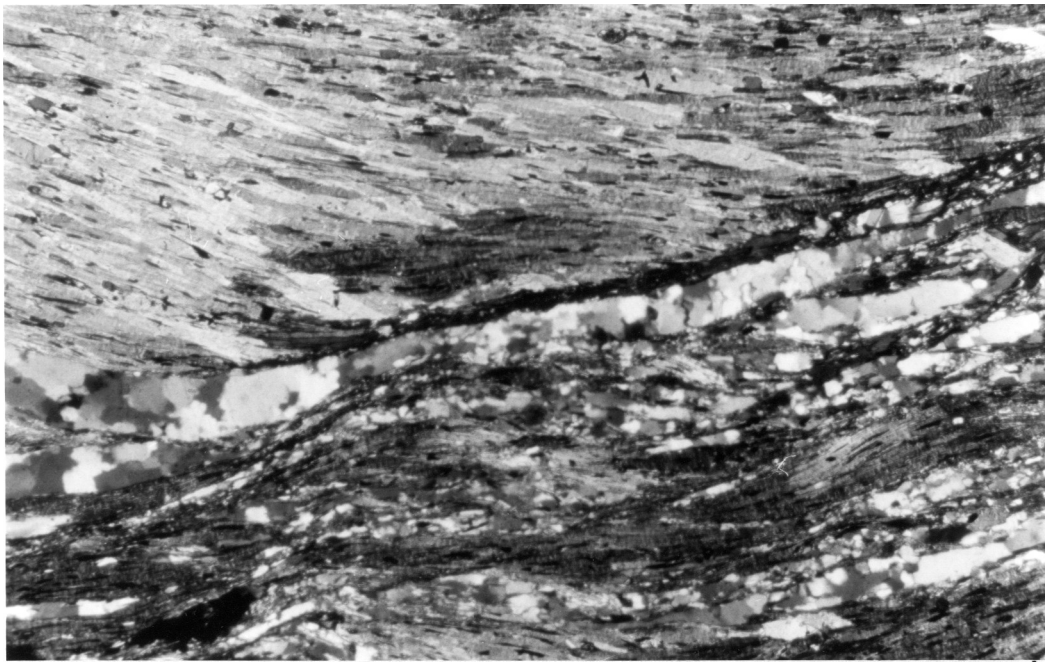

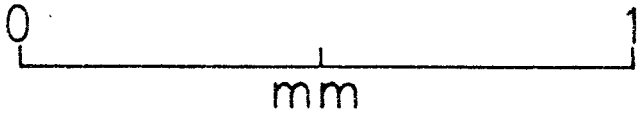

FIGURE 4-9D

FIGURE 4-9E

FIGURE 4-10. - Stretched pyrite grain in oblique cleavage. Pyrite grains with this shape are rare in the mylonite outside of cleavage zones. The grain appears to have been pulled apart in segments parallel to cleavage. AB81-94-3, 40X, PPL.

FIGURE 4-10

FIGURE 4-11. - Discrete oblique cleavage. Sample from Ripshin Mountain mylonite zone. Cleavage defined by fine chlorite, sericite, and minor quartz zones crossing from lower left to upper right of photograph. AB81-111, 25X, PX.

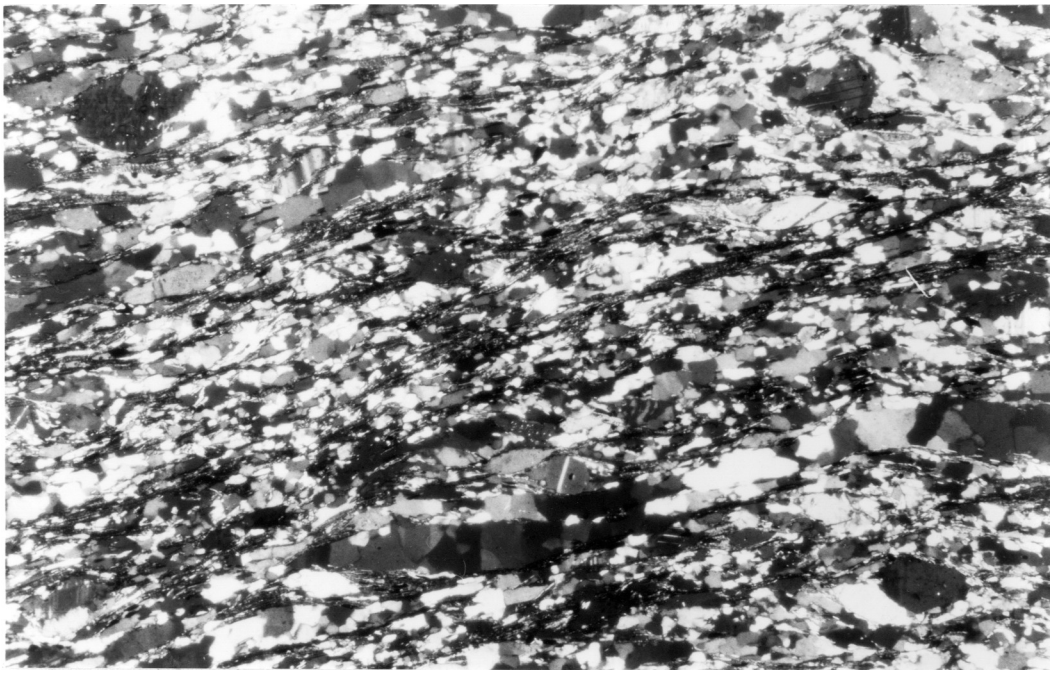

FIGURE 4-11